UNIVERSITEIT GENT

FACULTEIT INGENIEURSWETENSCHAPPEN

# *State-of-the-art Antenna Systems in Mobile Communications*

Hendrik Rogier

Roald Goossens, Carla Hertleer, Anneleen Tronquo

Information Technology Department – Electromagnetics Group

## Outline – Antenna theory

- **Introduction:**
  - Trends in mobile communications
- **Mutual coupling models for antenna arrays**
  - Impedance matrix, open-circuit voltage
  - Active element pattern
  - Dedicated models for uniform circular arrays (UCA)
    - **Phase modes**
    - **Coupling matrix**
    - **Spherical modes**
    - **Double Fourier transform**
    - **Spherical waves**
  - Dedicated model for UCA with center element



UNIVERSITEIT GENT

## Outline - Applications

- **Direction-of-arrival (DOA) estimation**
  - Active element MUltiple-SIgnal Classification (MUSIC) algorithm
  - DOA-estimation with UCAs
    - **In azimuth: real-beamspace root-MUSIC**
    - **In azimuth and elevation: UCA-RARE + root-MUSIC**
- **Performance of MIMO-systems**
  - Effect of antenna correlation in UCAs



## Outline – New antennas

- **Design of wearable antennas**
  - Conductive and non-conductive textile materials
  - Antenna characteristics
  - Effect of bending
  - Presence of human body
- **Conclusions**

## Trends in mobile communications

- **Broadband wireless applications for a wide range of mobile users require larger mobile channel capacity**
- **Advanced modulation and coding schemes (e.g. Turbo coding) have reached theoretical limit (Shannon capacity)**
- **Multi-antenna systems (antenna array + signal processing) increase the Shannon capacity and accommodate more broadband wireless users**
- **Antennas and propagation characteristics of the wireless link must be included to obtain optimal performance**
- **Antenna systems should be compact, flexible and integrated in the complete system, making them invisible to the mobile user**



## Mutual coupling in wireless systems

- **Antenna arrays suffer from mutual coupling and shadowing effects due to near-field scatterers**
  - Accurate but efficient antenna array models required!
- **Mutual coupling models for antenna arrays**
  - Impedance matrix, open-circuit voltage
  - Active element pattern
  - Dedicated models for uniform circular arrays (UCA)
    - **Phase modes**
    - **Coupling matrix**
    - **Spherical modes**
    - **Double Fourier transform**
    - **Spherical waves**
  - Dedicated model for UCA with center element

- **Transmit mode: impedance matrix, radiation pattern**
  - Geometry of ULA/UCA with two antenna elements

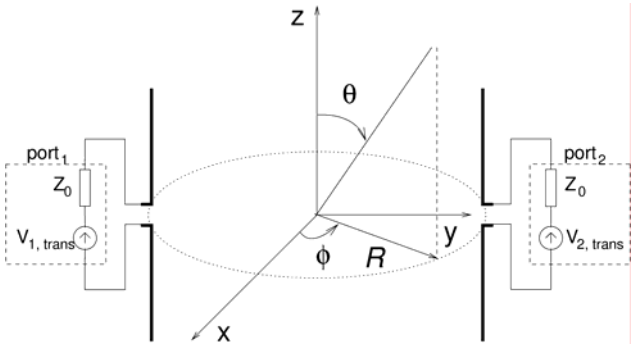






- **Transmit mode: impedance matrix, radiation pattern**
  - Circuit equivalent for two antenna element ULA/UCA

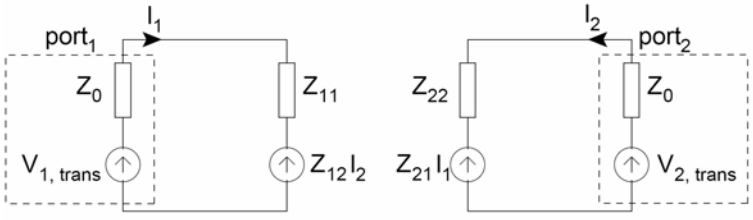


  - circuit elements: At each port *i* :
    1. antenna radiation impedance $Z_{ii}$
       (≠ radiation impedance of stand-alone element)
    2. voltage source $Z_{ij}\, I_j$ proportional to current in other antenna element *j*
  - elements found by exciting each port with **1A current source**
    + other ports **0A** (open circuited)
    → radiation pattern $\mathbf{F}_i(\theta, \phi)$ at each port *i*

## Mutual coupling models for antenna arrays

- **Transmit mode: impedance matrix, open-circuit voltage**
  - Circuit equivalent for two antenna element ULA/UCA

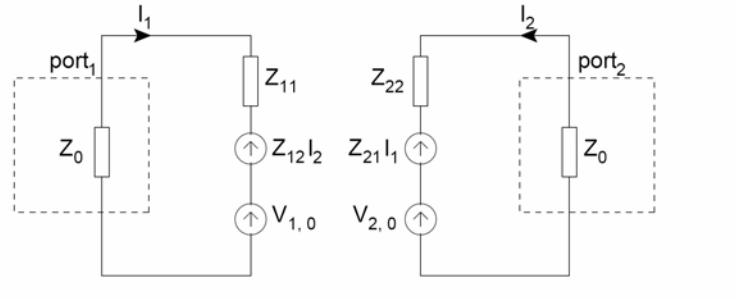


  - Invoking reciprocity yields at each port *i* :
    1. identical impedances $Z_{ij}$ as in transmit mode
    2. open-circuit voltage $V_{i,0}$ related to radiation pattern $\mathbf{F}_i(\theta, \phi)$:

$$V_{i,0}(\theta,\phi) = -\frac{2j\lambda}{R_e}\mathbf{E}^{\text{isc}}(\theta,\phi)\cdot\mathbf{F}_i(\theta,\phi)$$



## Mutual coupling models for antenna arrays

- **Active element pattern**

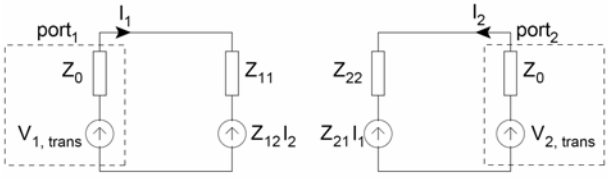


  - Radiation pattern
    - **Ideal current sources as feeds at antenna terminals**
    - **1A current source at one antenna terminal**
    - **Other terminals open-circuited**

    → **not very physical at high frequencies**
  - Active element pattern
    - **Thévenin equivalent for feeds at antenna terminals**
    - **1V voltage source + $Z_0$ at one antenna terminal**
    - **Others terminals terminated by load $Z_0$**

## Mutual coupling models for antenna arrays

- **Dedicated model for uniform circular arrays**
  - Geometry of a UCA

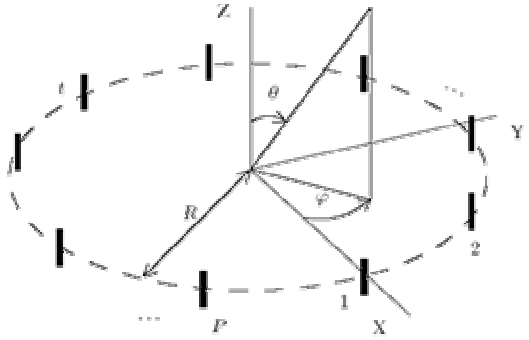


  - P identical elements
  - rotational invariance:
    $V_{i,0}(\theta, \phi) = V_{1,0}(\theta, \phi - 2\pi/P)$ + circulant impedance matrix $\overline{\overline{Z}}$



## Mutual coupling models for antenna arrays

- **Dedicated model for uniform circular arrays**
  - Phase modes
    - Expand radiation pattern and open-circuit voltages into Fourier series of phase-modes in $\phi$:

$$\mathbf{F}_i(\theta,\phi) = \sum_{m=-M}^{+M} \mathbf{F}_{i,m}^{\phi}(\theta) e^{jm\phi}$$

$$V_{1,0}(\theta,\phi) = \sum_{m=-M}^{+M} V_{0,m}^{\phi}(\theta) e^{jm\phi}$$

    - Rotational symmetry yields

$$\mathbf{F}_j(\theta,\phi) = \mathbf{F}_i(\theta,\phi-\phi_j+\phi_i) = \sum_{m=-M}^{+M} \mathbf{F}_{i,m}^{\phi}(\theta) e^{jm(\phi-\phi_j+\phi_i)}$$

- **Dedicated model for uniform circular arrays**
  - Phase modes
    - Fourier series expansion reduces impedance matrix $\overline{\overline{Z}}$ to phase-sequence impedances

$$Z_m^{\phi} = \sum_{l=1}^{L} Z_{i,l} e^{-jm\frac{2\pi(i-l)}{L}}$$

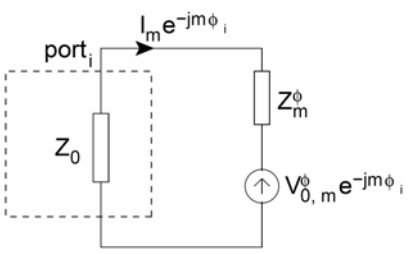


- phase-mode voltages $V_{0,m}^{\phi}$ and phase-sequence impedances $Z_m^{\phi}$ independent of port number $i$
- no coupling between models for different mode order $m$





- **Dedicated model for uniform circular arrays**
  - Phase modes for the scalar case
    - Simplifications
      - currents on antenna elements $z$-oriented: current density $\mathbf{C}(r,\phi,z) = C(r,\phi,z)\mathbf{u}_z$
      - radiation pattern in azimuth (xy-)plane z-oriented + linear polarization: $\mathbf{F}_i(\theta,\phi) = F_i(\phi)\mathbf{u}_z$

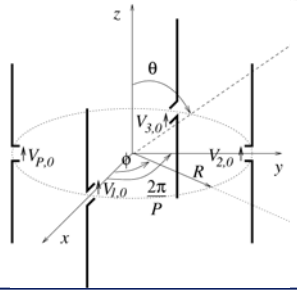

- **Dedicated model for uniform circular arrays**
  - Phase modes for the scalar case
    - Following property holds between far-field and antenna-current on aperture with radius $R$=$r$:

$$F_m^{\phi}(\theta) = -\frac{j\omega\mu_0 \sin\theta}{2\pi} \int_{\phi=0}^{2\pi} \int_{\phi'=0}^{2\pi} \int_z C(r,\phi',z) e^{jk_0(r\sin\theta\cos(\phi-\phi')+z\cos\theta)} e^{-jm\phi}\, d\phi' dz d\phi$$

$$= -j^{m-1}\omega\mu_0 \sin\theta J_m(k_0 r\sin\theta) \int_{\phi'=0}^{2\pi} \int_z C(r,\phi',z) e^{-jm\phi'} e^{jk_0 z\cos\theta}\, d\phi' dz$$

1. phase-mode component $F_m^{\phi}$ relates to phase mode current component of same order
2. $|F_m^{\phi}|$ quickly decreases when phase-mode order $m > k_0 R$





- **Dedicated model for uniform circular arrays**
  - Number of phase modes
    - An accurate description is obtained when the number of phase modes is much larger than the electrical dimensions of the UCA: $M >> k_0 R$ ($k_0 = 2\pi/\lambda$)

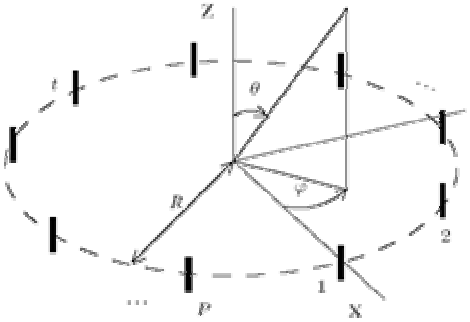


$$\mathbf{F}_i(\theta,\phi) = \sum_{m=-M}^{+M} \mathbf{F}_{i,m}^{\phi}(\theta) e^{jm\phi}$$

$$V_{1,0}(\theta,\phi) = \sum_{m=-M}^{+M} V_{0,m}^{\phi}(\theta) e^{jm\phi}$$

- **Dedicated model for uniform circular arrays**
  - **Example 1: Array of two vertical dipoles**
    - two thin-dipole antennas tuned to 900MHz (dipole length $l = 16.12$cm)
    - element spacing $\delta = \frac{l}{5} (\approx \frac{\lambda}{10})$:

$$\overline{\overline{Z}} = \begin{pmatrix} (73.058600 - 1.215010j)\Omega & (67.785100 + 2.539880j)\Omega \\ (67.785100 + 2.539880j)\Omega & (73.058600 - 1.215010j)\Omega \end{pmatrix}$$

    - element spacing $\delta = l (\approx \frac{\lambda}{2})$:

$$\overline{\overline{Z}} = \begin{pmatrix} (72.531900 + 1.368460j)\Omega & (-12.124400 - 30.453400j)\Omega \\ (-12.124400 - 30.453400j)\Omega & (72.531900 + 1.368460j)\Omega \end{pmatrix}$$

    → $Z_{12}$ larger for smaller spacing between antennas





- **Dedicated model for uniform circular arrays**
  - **Example 1: Array of two vertical dipoles**

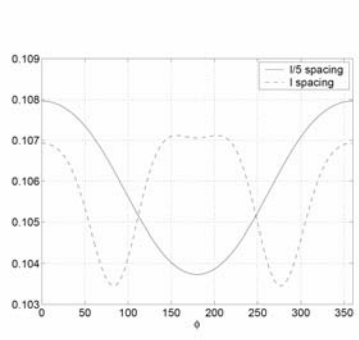


Open-circuit voltage $|V_{0,1}|$

→ pattern not fully omnidirectional!

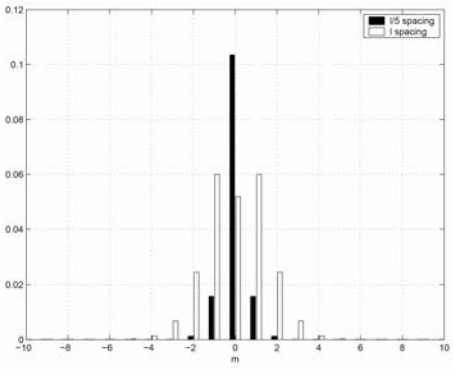


Phase mode voltages $|V_{0,m}^{\phi}|$

→ # relevant pase modes ↗ when spacing ↗

- **Dedicated model for uniform circular arrays**
  - Construction of a coupling matrix
    - All ports loaded by termination $Z_0$

$$V_{Z_0,m}^{\phi}(\theta) = \frac{Z_0}{Z_m^{\phi} + Z_0} V_{0,m}^{\phi}(\theta)$$

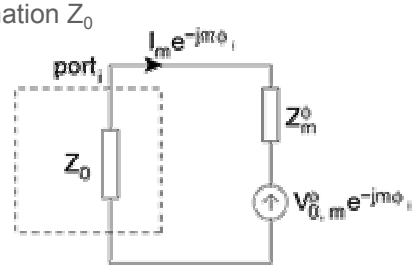


    - Response of ideal array

$$\mathbf{V}_{Z_0}^{(NC)}(\phi,\theta) = \mathbf{V}_0^{(1)}(\phi,\theta)$$

$$\left(e^{jk_0 r\cos(\phi)}, e^{jk_0 r\cos(\phi-\frac{2\pi}{N_c})}, \ldots, e^{jk_0 r\cos(\phi-\frac{2(N_c-1)\pi}{N_c})}\right)^T$$





- **Dedicated model for uniform circular arrays**
  - Relate ideal array response to real array response
    - **θ fixed !!**
    - **For each phase mode m, we define** $Z_m^{\phi,(MC)}$

$$V_{Z_0,m}^{\phi}(\theta) = \frac{Z_0}{Z_m^{\phi} + Z_0} V_{0,m}^{\phi}(\theta) = \frac{Z_0}{Z_m^{\phi,(MC)} + Z_0} V_{0,m}^{\phi,(NC)}$$

    - **Definition coupling matrix** $\overline{\overline{C}}$

$$\mathbf{V}_{Z_0}(\phi,\theta) = \overline{\overline{C}} \cdot \mathbf{V}_{Z_0}^{(NC)}(\phi,\theta)$$

$$= Z_0(\overline{\overline{Z}}_{MC} + Z_0\overline{\overline{I}})^{-1} \cdot \mathbf{V}_{Z_0}^{(NC)}(\phi,\theta)$$

    - ***Accurate compensation for mutual coupling when number of elements in UCA sufficiently large***

- **Dedicated model for uniform circular arrays**
  - Spherical modes for the scalar case
    - Expand phase mode components $F_m^{\phi}$ into series of associated Legendre polynomials

$$F_m^{\phi}(\theta) = \sin\theta \sum_{n=0}^{+\infty} F_{m,n}^{\phi,\theta} P_n^{|m|}(\cos\theta)$$

    - Relation between current density and radiation pattern

$$F_{m,n}^{\phi,\theta} = -j^{m-1}\omega\mu_0 \int_{\phi'=0}^{2\pi}\int_z C(r,\phi',z)\left[\int_{\theta=0}^{\pi} J_m(k_0 r\sin\theta)e^{jk_0 z\cos\theta}P_n^{|m|}(\cos\theta)\sin\theta d\theta\right]e^{-jm\phi}\,d\phi' dz$$

$$= (-1)^{\frac{n}{2}}(-j)^{m-1}\omega\mu_0 \int_{\phi'=0}^{2\pi}\int_z C(r,\phi',z) j_n(k_0\sqrt{r^2+z^2})P_n^{|m|}(\frac{z}{\sqrt{r^2+z^2}})e^{-jm\phi}\,d\phi' dz$$

    - Number of spherical modes $N$ limited by electrical dimensions of UCA: $N >> k_0\sqrt{r^2+z_{\max}^2}$





- **Dedicated model for uniform circular arrays**
  - Spherical modes for the scalar case
    - Expansion of radiation pattern

$$F(\phi,\theta) = \sin\theta \sum_{m=-M}^{+M}\sum_{n=0}^{+N} F_{m,n}^{\phi,\theta} P_n^{|m|}(\cos\theta)e^{jm\phi}$$

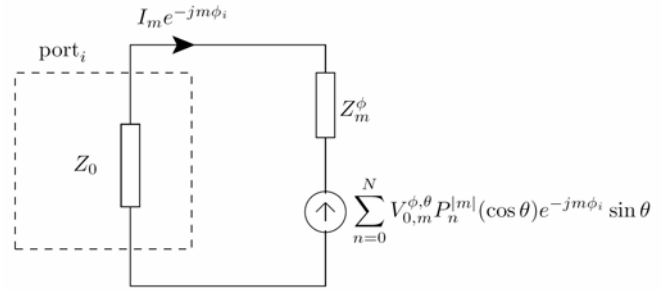

- **Dedicated model for uniform circular arrays**
  - Example 2: Nine vertical dipoles in UCA constellation

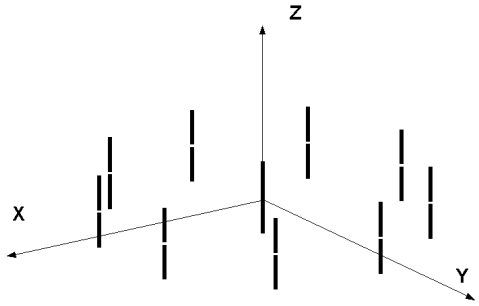


- **frequency: 900 MHz**
- **R=λ/4**
- **dipole length l = 16.12cm ≈ λ/2**
- **additional short-circuited dipole (platform effect)**





- **Dedicated model for uniform circular arrays**
  - Example 2: Nine vertical dipoles in UCA constellation

spherical-mode coefficients $|F^{TE,\Phi}_{n,m}|$

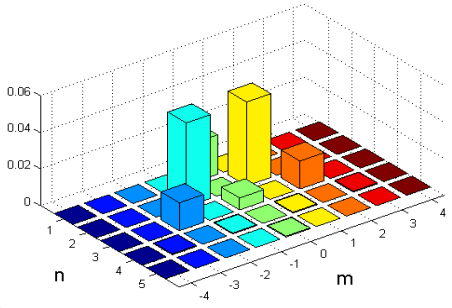


- **M ≈ 4 N ≈ 3**
- **36 coefficients describe EM-behavior UCA in full detail at all antenna ports**

- **Dedicated model for uniform circular arrays**
  - Phase-mode expansion in $\theta$ for the scalar case
    - Define the modified radiation pattern:

$$G(\theta,\varphi) = \begin{cases} F(\theta,\varphi) & \text{when} \quad 0<\theta<\pi \quad 0<\varphi<\pi \\ -F(2\pi-\theta,\pi+\varphi) & \text{when} \quad \pi<\theta<2\pi \end{cases}$$

    - Now expand $\theta$ into Fourier series

$$G(\theta,\varphi) = \sum_{n=-\infty}^{n=+\infty} g_n(\varphi) e^{jn\theta}$$

    - Following identity holds ($\alpha = k\sqrt{z^2 + R^2\cos(\varphi-\varphi')^2}$)

$$g_n(\varphi) = \frac{j^{n-1}}{2j}\int_{\varphi'}\int_{z} C(R,\varphi',z)(J_{n-1}(\alpha)e^{-j(n-1)\beta} + J_{n+1}(\alpha)e^{-j(n+1)\beta})\mathrm{d}\varphi'\mathrm{d}z$$

      → decomposition into limited number of phase modes in θ for $N > k\sqrt{R^2+z_{max}^2}+1$





- **Dedicated model for uniform circular arrays**
  - Double Fourier expansion for the scalar case
    - Double Fourier expansion of modified radiation pattern:

$$G(\theta,\varphi) = \sum_{m=-M}^{M}\sum_{n=-N}^{N} f_{mn} e^{jm(\varphi-\varphi_t)} e^{jn\theta}$$

    - Limited number of terms $M$ and $N$

$$M > kR$$

$$N > k\sqrt{R^2+z_{max}^2}+1$$

- **Dedicated model for uniform circular arrays**
  - Example 2: Nine vertical dipoles in UCA constellation

double Fourier coefficients $|f_{mn}|$

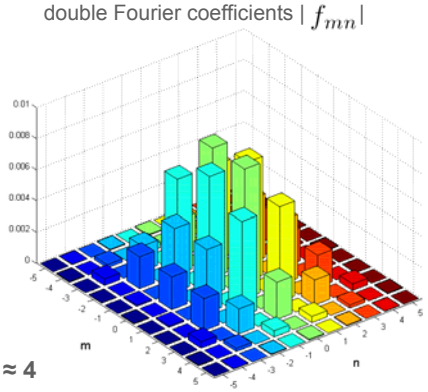


- **M ≈ 4; N+1 ≈ 4**
- **45 coefficients describe EM-behavior UCA in full detail at all antenna ports**





- **Dedicated model for uniform circular arrays**
  - Spherical-wave expansion of the radiation vector
    - Expansion for $\mathbf{F}_i(\phi,\theta) = (F_{i,\phi}(\phi,\theta), F_{i,\theta}(\phi,\theta))$

$$F^{\phi}_{\phi,m}(\theta) = j\sum_{n=1}^{+\infty}\left[A^{\phi,\theta}_{n,m}\frac{mP_n^{|m|}(\cos\theta)}{\sin\theta} + B^{\phi,\theta}_{n,m}\frac{dP_n^{|m|}(\cos\theta)}{d\theta}\right]$$

$$F^{\phi}_{\theta,m}(\theta) = \sum_{n=1}^{+\infty}\left[A^{\phi,\theta}_{n,m}\frac{dP_n^{|m|}(\cos\theta)}{d\theta} + B^{\phi,\theta}_{n,m}\frac{mP_n^{|m|}(\cos\theta)}{\sin\theta}\right]$$

    - Determination of spherical-wave coefficients

$$A^{\phi,\theta}_{n,m} = -\frac{(2n+1)(n-|m|)!}{2n(n+1)(n+|m|)!}\int_{\theta=0}^{\pi}\left[jmF^{\phi}_{\phi,m}(\theta)P_n^{|m|}(\cos\theta) - F^{\phi}_{\theta,m}(\theta)\frac{dP_n^{|m|}(\cos\theta)}{d\theta}\sin\theta\right]d\theta$$

$$B^{\phi,\theta}_{n,m} = j\frac{(2n+1)(n-|m|)!}{2n(n+1)(n+|m|)!}\int_{\theta=0}^{\pi}\left[-F^{\phi}_{\phi,m}(\theta)\frac{dP_n^{|m|}(\cos\theta)}{d\theta}\sin\theta - jmF^{\phi}_{\theta,m}(\theta)P_n^{|m|}(\cos\theta)\right]d\theta.$$

- **Dedicated model for uniform circular arrays**
  - Spherical-wave expansion of the open-circuit voltage
    - **Horizontally polarized incoming plane wave (unit amplitude)**

$$V_{i,0}^{\mathrm{H}}(\theta,\phi) = \sum_{m=-M}^{+M} V_{0,m}^{\mathrm{H},\phi}(\theta) e^{jm\phi}$$
$$= \frac{2\lambda}{R_c} \sum_{n=1}^{N} \left[ \sum_{m=-n}^{+n} \left( A_{n,m}^{\phi,\theta} \frac{m P_n^{|m|}(\cos\theta)}{\sin\theta} + B_{n,m}^{\phi,\theta} \frac{dP_n^{|m|}(\cos\theta)}{d\theta} \right) \right] e^{jm\phi}$$

    - **Vertically polarized incoming plane wave (unit amplitude)**

$$V_{i,0}^{\mathrm{V}}(\theta,\phi) = \sum_{m=-M}^{+M} V_{0,m}^{\mathrm{V},\phi}(\theta) e^{jm\phi}$$
$$= -\frac{2j\lambda}{R_c} \sum_{n=1}^{N} \left[ \sum_{m=-n}^{+n} \left( A_{n,m}^{\phi,\theta} \frac{dP_n^{|m|}(\cos\theta)}{d\theta} + B_{n,m}^{\phi,\theta} \frac{m P_n^{|m|}(\cos\theta)}{\sin\theta} \right) \right] e^{jm\phi}$$





- **Dedicated model for uniform circular arrays**
  - Example 3: Four-element array of tilted dipoles

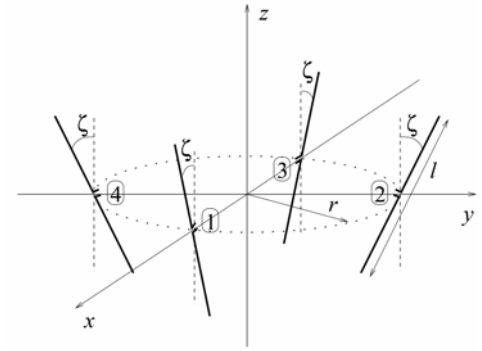


    - **frequency: 900 MHz**
    - **Distance between adjacent elements = 0.86 λ**
    - **dipole length l = 16.12cm ≈ λ/2**

- **Dedicated model for uniform circular arrays**
  - Example 3: Four-element array of tilted dipoles

tilt angle $\zeta = 0°$

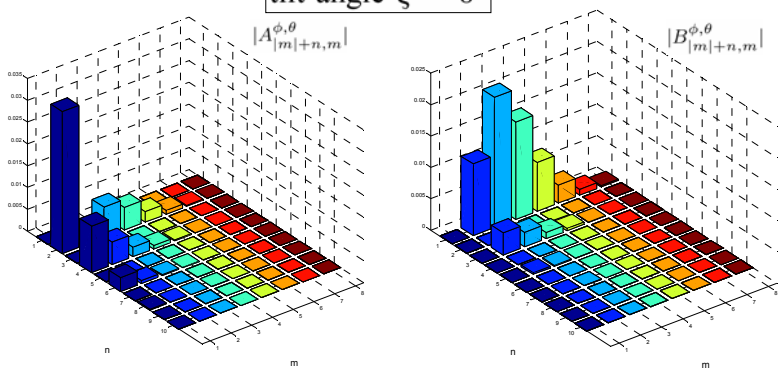


- **Symmetry:** $A^{\phi,\theta}_{|m|+n,m} = 0$, for $n$ even, $B^{\phi,\theta}_{|m|+n,m} = 0$, for $n$ odd





- **Dedicated model for uniform circular arrays**
  - Example 3: Four-element array of tilted dipoles

tilt angle $\zeta = 30°$

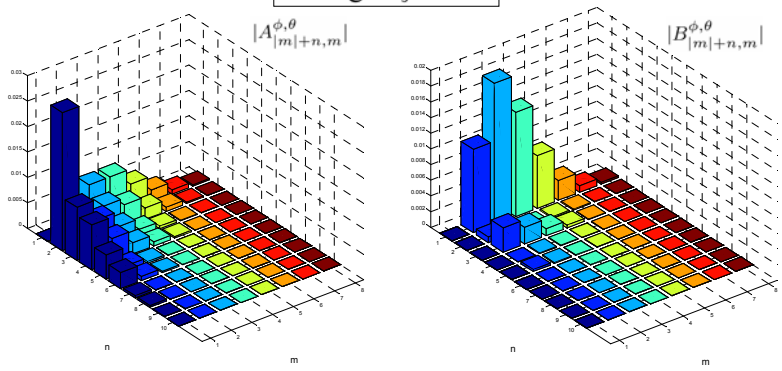


- **Overall dimensions increase as tilt angle increases**
  **→ components with larger *m* and *n* values gain in importance**

- **Dedicated model for uniform circular arrays**
  - Example 3: Four-element array of tilted dipoles

$$\text{tilt angle } \zeta = 75°$$

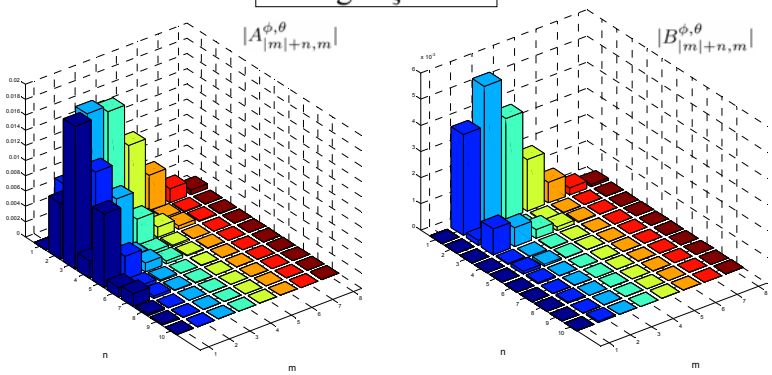


- **Relevant coefficients for -7 ⪯ m ⪯ 7 and 0 ⪯ n ⪯ 9**
  **→ 150 coefficients describe all coupling effects**





- **Dedicated model for uniform circular arrays**
  - Example 3: Four-element array of tilted dipoles

$$\text{tilt angle } \zeta = 90°$$

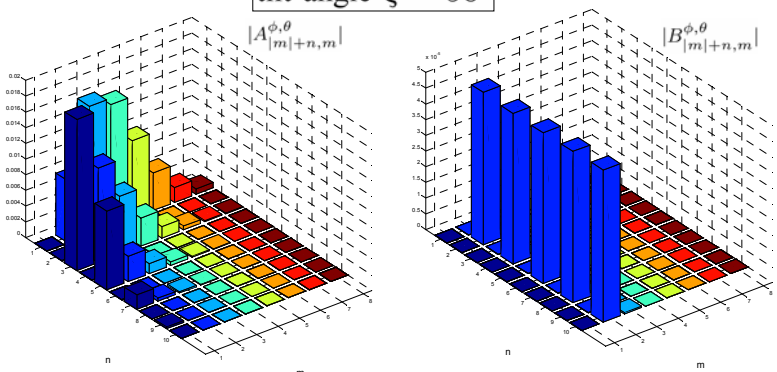


- **Symmetry:** $A^{\phi,\theta}_{|m|+n,m} = 0$, for $n$ odd, $B^{\phi,\theta}_{|m|+n,m} = 0$

## Dedicated model for uniform circular arrays

- Number of spherical-wave coefficients
  - **Rule of thumb for 0.1% accuracy**

$$N = \lceil 4\frac{d}{\lambda} + 4 \rceil$$

  - **Total number of spherical-wave coefficients**

$$2(\lceil 4\frac{d}{\lambda} + 4 \rceil)(\lceil 4\frac{d}{\lambda} + 6 \rceil)$$

  - **Examples**
    - d = λ : 160 coefficients
    - d = 2λ : 336 coefficients
    - Classical approach: 2×360×180 coefficients





## Dedicated model for UCA with center element

- Geometry of UCA with center element
  - **P-1 identical outer elements:**
    **- labels 2, …, P**
    **- rotational symmetry**

$$V_{0,i}(\theta,\phi) = V_{0,2}(\theta,\phi-(i-2)\frac{2\pi}{P-1}$$
$$i = 2,\ldots,P.$$

  - **center element:**
    **- label 1**
    **- rotational symmetry**

$$V_{0,1}(\theta,\phi) = V_{0,1}(\theta,\phi-\frac{2\pi}{P-1})$$

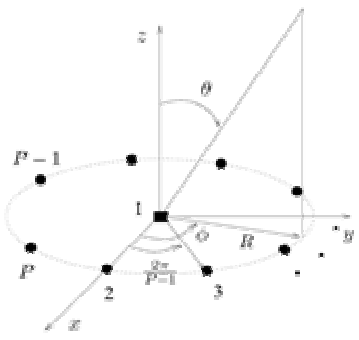

## Dedicated model for UCA with center element

- Impedance matrix $\overline{\overline{Z}}$ :

$$\overline{\overline{Z}} = \left( \begin{array}{c|c} Z_{1,1} & Z_{1,2}\mathbf{I}_{1\times(N-1)} \\ \hline Z_{1,2}\mathbf{I}_{(N-1)\times 1} & \overline{\overline{Z}}_{\text{outer}} \end{array} \right)$$

  - $\overline{\overline{Z}}_{\text{outer}}$ **is a circulant matrix**

- Phase-mode decomposition of voltages and impedances

$$V_{0,i}(\theta,\phi) = \sum_{m=-M}^{+M} V_{0,i,m}^{\phi}(\theta) e^{jm\phi} \qquad M = \lceil 4\frac{d}{\lambda} + 4 \rceil$$

$$Z_{\text{outer},m}^{\phi} = \sum_{n=1}^{N-1} Z_{\text{outer},i-1,n} e^{-j\frac{2\pi m(i-1-n)}{N-1}}$$

- center element only contributes to modes of order $l$ ($P$ - 1)





## Dedicated model for UCA with center element

- Circuit model in receive mode
  - **for phase modes of the orders $l$ ( $P$ − 1) (l = 0, 1, . . .).**

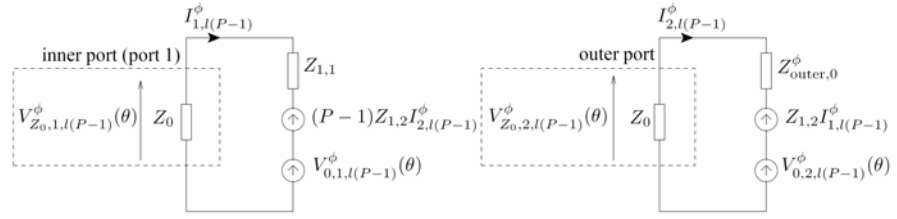


  - **Coupling between center element and outer antennas**

## Mutual coupling models for antenna arrays

- **Dedicated model for UCA with center element**
  - Circuit model in receive mode
    - **for phase modes of the order $m$, different from $l$ ( $P - 1$).**

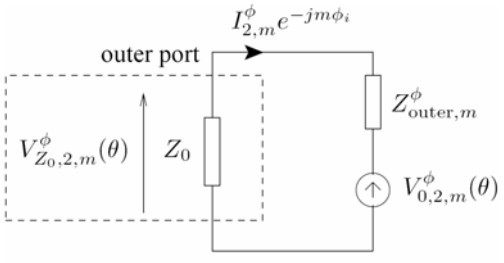


    - **no coupling between center element and outer antennas**



## Smart antenna and MIMO systems

- **Accounting for real antenna characteristics increases performance of smart antenna and MIMO systems**
- **Direction-of-arrival (DOA) estimation**
  - Active element MUltiple-SIgnal Classification (MUSIC) algorithm
  - DOA-estimation with UCAs
    - **In azimuth: real-beamspace root-MUSIC**
    - **In azimuth and elevation: UCA-RARE + root-MUSIC**
- **Performance of MIMO-systems**
  - Effect of antenna correlation in UCAs

## Direction-of-arrival estimation

- **Active element MUSIC algorithm**
  - Consider $L$ source signals $s_l(n)$ impinging on the array from DOAs $(\theta, \phi_l)$ in presence of AWGN $\mathbf{n}(n)$
  - Data samples $\mathbf{x}(n)$ at antenna terminals (all loaded by $Z_0$):

$$\mathbf{x}(n) = \sum_{l=1}^{L} \mathbf{V}_{Z_0}(\theta, \phi_l) s_l(n) + \mathbf{n}(n)$$

  - Definition of SNR!
    - Signal processing definition only includes receiver noise (no antenna characteristics)

$$\mathrm{SNR} = \frac{\mathrm{E}[|\mathrm{V}_{Z_0,\mathrm{j}}(\mathrm{n})|^2]}{\mathrm{E}[|\mathrm{n_j}(\mathrm{n})|^2]}$$

    - We include effects of mismatch

$$\mathrm{SNR} = \frac{\mathrm{E}[|\mathrm{V}_{0,\mathrm{j}}(\mathrm{n})|^2]}{\mathrm{E}[|\mathrm{n_j}(\mathrm{n})|^2]}$$

*open-circuit voltage* $\mathrm{V}_{0,\mathrm{j}} > \mathrm{V}_{Z_0,\mathrm{j}}$



## Direction-of-arrival estimation

- **Active-element MUSIC algorithm**
  - Data correlation matrix $\overline{\overline{R}}_x = E[\mathbf{x}(n)\mathbf{x}^H(n)]$
  - Eigenvalue decomposition or SVD yields

$$\overline{\overline{R}}_x = \overline{\overline{E}}_S \cdot \overline{\overline{\Lambda}}_S \cdot \overline{\overline{E}}_S^H + \overline{\overline{E}}_N \cdot \overline{\overline{\Lambda}}_N \cdot \overline{\overline{E}}_N^H$$

$\overline{\overline{E}}_S$: signal subspace : $\mathrm{Span}\,\overline{\overline{E}}_S = \mathrm{Span}\,[\mathbf{V}_{Z_0}(\theta, \phi_1), \ldots, \mathbf{V}_{Z_0}(\theta, \phi_L)]$
$\overline{\overline{\Lambda}}_S$: diagonal matrix containing signal powers
$\overline{\overline{E}}_N$: noise subspace :
$\overline{\overline{\Lambda}}_N$: diagonal matrix containing noise powers

  - $\overline{\overline{E}}_N \perp \overline{\overline{E}}_S \Rightarrow \mathbf{V}_{Z_0}(\theta, \phi) \cdot \overline{\overline{E}}_N = 0$ for $\phi = \phi_l$
  - DOAs found as peaks in MUSIC spectrum

$$P_{\mathrm{MUSIC}}(\theta, \phi) = \frac{1}{\left| \mathbf{V}_{Z_0}(\theta, \phi) \cdot \overline{\overline{E}}_N \right|^2}$$

## Direction-of-arrival estimation

- **Example: Planar array**

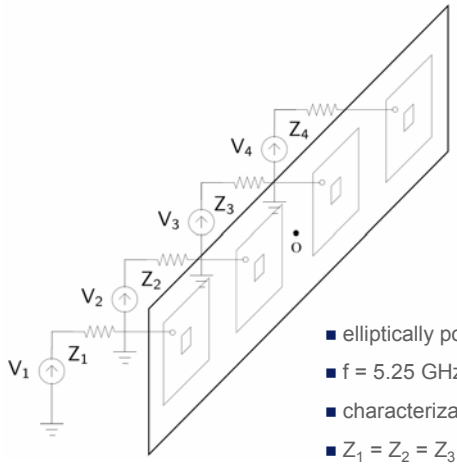


- elliptically polarized patch antennas
- f = 5.25 GHz
- characterization through active element patterns
- $Z_1 = Z_2 = Z_3 = Z_4 = Z_0$



## Direction-of-arrival estimation

- **Effect of mutual coupling on DOA estimation**

- MUSIC spectrum for three arrays with different spacings between the elements:

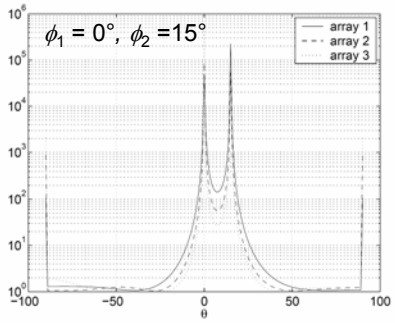


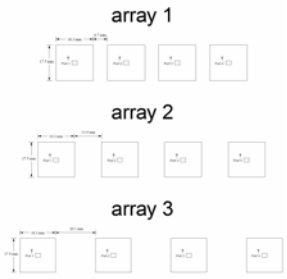


- correct DOA estimates in the presence mutual coupling, finer peaks for larger arrays

## DOA estimation of ϕ with UCAs

- **Compact description of EM coupling effects**
  - Coupling matrix $\overline{\overline{C}}$ for fixed elevation angle

$$\mathbf{V}_{Z_0}(\phi,\theta) = \overline{\overline{C}} \cdot \mathbf{V}_{Z_0}^{(NC)}(\phi,\theta)$$

    - **Dimensions : $N_e$ x $N_e$ ($N_e$ = number of array elements)**
    - **Description only accurate for $N_e$ >> electrical dimensions array**
  - DOAs found as peaks in MUSIC spectrum

$$P_{\text{MUSIC}}(\theta,\phi) = \frac{1}{\left|\overline{\overline{C}} \cdot \mathbf{V}_{Z_0}^{(NC)}(\theta,\phi) \cdot \overline{\overline{E}}_N\right|^2}$$



## DOA estimation of ϕ with UCAs

- **Example: Dual-band UCA**

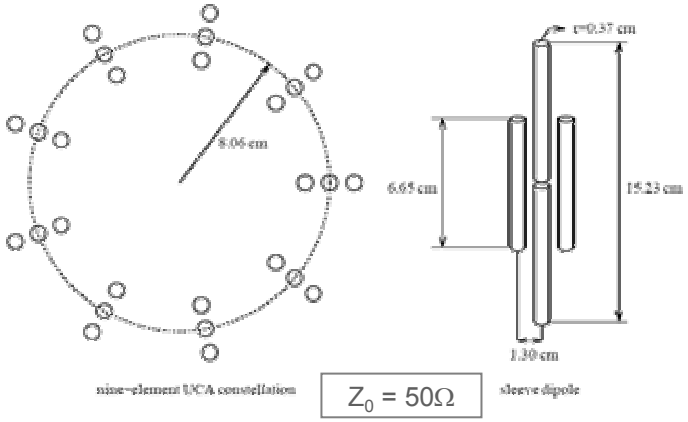


$Z_0 = 50\Omega$

**Antennas matched to 900 MHz and 1800 MHz**

## DOA estimation of $\phi$ with UCAs

- **Coupling matrix for UCA with 9 elements**

900 MHz

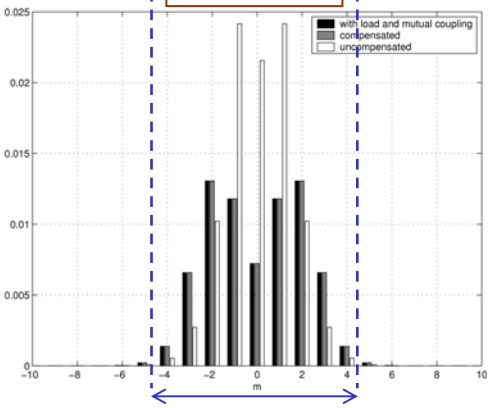


*Corrected by coupling matrix*

- **Compensation for phase mode orders - 4 ⊙ m ⊙ 4**
- **All relevant components included**
- **Example: 2 DOAs**
  - $\phi_1 = 55°$, $\phi_2 = 65°$
  - equal source power
  - 10000 bit pseudo-random sequences, SNR = 10 dB
  - Ensemble of 500 sequences
  - Estimates: $\hat{\phi}_1 = 55.02°$, $\hat{\phi}_2 = 64.97°$



## DOA estimation of $\phi$ with UCAs

- **Coupling matrix for dual-band UCA**

1800 MHz

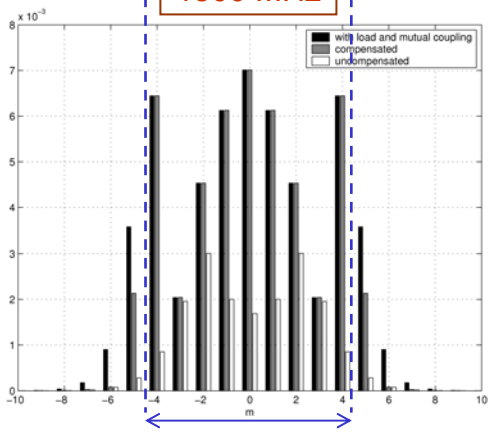


*Corrected by coupling matrix*

- **Compensation for phase mode orders - 4 ⊙ m ⊙ 4**
- **Not all relevant components included**
- **Example: 2 DOAs**
  - $\phi_1 = 55°$, $\phi_2 = 65°$
  - 9 elements: no peaks found
  - 11 elements: $\hat{\phi}_1 = 56.0°$, $\hat{\phi}_2 = 63.9°$
  - 13 elements: $\hat{\phi}_1 = 55.0°$, $\hat{\phi}_2 = 65.0°$

*Improved mutual coupling compensation by increasing number of elements*

## DOA estimation of $\phi$ with UCAs

- **Real beamspace MUSIC algorithm for UCAs**
  - Exciting phase modes in a UCA

- $N$ element UCA can excite phase modes up to the order $\lfloor \frac{N-1}{2} \rfloor$
- beamforming vector for phase mode $m$:

$$\mathbf{w}_m^H = \frac{1}{N}\left[1, e^{j\frac{2\pi m}{N}}, \ldots, e^{j\frac{2\pi(N-1)m}{N}}\right]$$

- according to Nyquist's sampling theorem, far-field pattern is not monomodal, but

$$\mathsf{F}_m^w(\theta) = \sum_{k=-\infty}^{+\infty} \mathsf{F}_{1,m+Nk}^{\phi}(\theta) e^{j(m+Nk)\phi}$$

- $\mathsf{F}_m^w(\theta) \approx \mathsf{F}_{1,m}^{\phi}$ for $N \gg k_0 r$



## DOA estimation of $\phi$ with UCAs

- **Real beamspace MUSIC algorithm for UCAs**
  - Beamspace transformation of data vector

$$\mathbf{y}(t) = \overline{\overline{W}}^H \overline{\overline{C}}_v(\theta) \overline{\overline{V}}^H \mathbf{x}(t)$$

$$\overline{\overline{V}} = \sqrt{N_e}\left[\mathbf{w}_{-M} \vdots \cdots \vdots \mathbf{w}_0 \vdots \cdots \vdots \mathbf{w}_M\right]$$

$$\overline{\overline{C}}_v(\theta) = \mathrm{diag}[e^{-j\angle V_{0,M}^{\phi}(\theta)}, \ldots, e^{-j\angle V_{0,M}^{\phi}(\theta)}]$$

$$\overline{\overline{W}} = \frac{1}{\sqrt{M'}}\left[\mathbf{v}(\alpha_{-M}) \vdots \cdots \vdots \mathbf{v}(\alpha_0) \vdots \cdots \vdots \mathbf{v}(\alpha_M)\right]$$

$$\mathbf{v}(\phi) = \left[e^{-jM\phi}, \ldots, e^{jM\phi}\right] \qquad M' = 2M+1 \text{ and } \alpha_i = \frac{2\pi i}{M'}$$

1. $\overline{\overline{V}}$ uses beamformers $\mathbf{w}_m$ to transform to phase-mode voltages $V_{0,m}^{\phi}$, (in case of load $Z_0$: $\frac{Z_0}{Z_0+Z_m^{\phi}} V_{0,m}$)
2. $\overline{\overline{C}}_v(\theta)$ transforms to a centro-Hermitian ($X_{N+1-i} = X_i^*, i = 1, \ldots, N$) manifold,
3. $\overline{\overline{W}}$ transforms to a real manifold $\mathbf{b}(\theta, \phi)$.

## DOA estimation of ϕ with UCAs

- **Real beamspace MUSIC algorithm for UCAs**
  - Noise subspace $\overline{\overline{E}}_N$ constructed by real eigenvalue decomposition of

$$Re(\overline{\overline{R}}_y) = Re(E[\mathbf{y}(t)\mathbf{y}^H(t)])$$

  - Real-valued beamspace manifold (open-circuit case)

$$\mathbf{b}(\theta,\phi) = [f(\theta,\phi-\alpha_{-M}),\ldots,f(\theta,\phi-\alpha_{-1}),f(\theta,\phi),$$
$$f(\theta,\phi-\alpha_1),\ldots,f(\theta,\phi-\alpha_M)]$$

$$f(\theta,\phi) = \sqrt{\tfrac{N}{M'}}[|V^{\phi}_{0,0}| + 2\textstyle\sum_{m=1}^{M}|V^{\phi}_{0,m}|\cos(m\phi)]$$

  - DOAs: peaks in MUSIC spectrum:

$$P_{\mathrm{RB-MUSIC}}(\theta,\phi) = \frac{1}{\left|\mathbf{b}(\theta,\phi)\cdot\overline{\overline{E}}_N\right|^2}$$



## DOA estimation of ϕ with UCAs

- **Real beamspace root-MUSIC for UCAs**
  - The MUSIC function $\left|\mathbf{b}(\theta,\phi)\cdot\overline{\overline{E}}_N\right|^2$ can be written as

$$V(\phi,\theta) = \sum_{l=-M'+1}^{M'-1} a_\theta(l)e^{jl\phi}$$

  - Setting $z = e^{j\phi}$ results in polynomial equation
  - roots $z_i$ closest to unit circle yield azimuth estimates for DOAs

$$\phi_i = \arg(z_i)$$

  - Extension of root-MUSIC to UCAs with mutual coupling
  - benefits from advantages of root-MUSIC,
    e.g. lower failure rate for closely spaced sources

## DOA estimation of ϕ with UCAs

- **Beamspace MUSIC with 9 element dual-band UCA**

Beamspace MUSIC spectrum @ 900 MHz

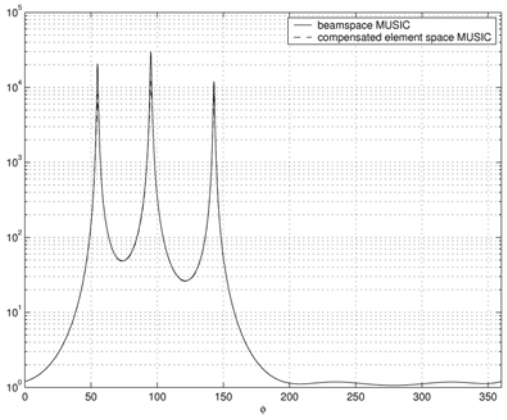


- **Compensation for phase mode orders - 4 ✪ m ✪ 4**
- **All relevant components included**
- **Example: 3 DOAs**
  - $\phi_1$= 55°, $\phi_2$= 95°, $\phi_3$= 143°
  - – equal source power
  - – 10000 bit pseudo-random sequences, SNR = 10 dB
  - – ensemble of 500 sequences
  - – accurate estimates with beamspace MUSIC and coupling matrix



## DOA estimation of ϕ with UCAs

- **Beamspace MUSIC with 9 element dual-band UCA**

Beamspace MUSIC spectrum @ 1800 MHz

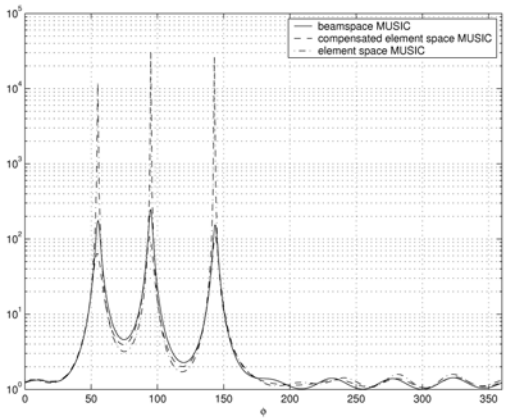


- **Compensation for phase mode orders - 4 ✪ m ✪ 4**
- **Not all relevant components included**
- **Example: 3 DOAs**
  - $\phi_1$= 55°, $\phi_2$= 95°, $\phi_3$= 143°
  - – equal source power
  - – 10000 bit pseudo-random sequences, SNR = 10 dB
  - – ensemble of 500 sequences
  - – inaccurate estimates with beamspace MUSIC and coupling matrix

## DOA estimation of $\phi$ with UCAs

- **Beamspace MUSIC with 9 element dual-band UCA**
  - Resolving power of root-MUSIC for UCAs

| | root MUSIC | | | comp MUSIC | | |
|---|---|---|---|---|---|---|
| $N_c$ | 9 | 11 | 13 | 9 | 11 | 13 |
| DOA 1 | 54.9°(0.6°) | 55.2°(0.04°) | 55.0°(0.03°) | - | 56.0°(3°) | 55.0°(3°) |
| DOA 2 | 65.1°(0.6°) | 63.5°(0.06°) | 65.0°(0.03°) | - | 63.9°(0.3°) | 65.0°(3°) |

TABLE V

DUALBAND UCA: MEAN AND STANDARD DEVIATION FOR DOA ESTIMATION AT 1880 MHz; INCOMING SIGNALS AT 55° AND 65°, WITH SNR=10dB.

| | root MUSIC | | | |
|---|---|---|---|---|
| $\delta$ | 2° | 3° | 4° | 5° |
| DOA 1 | 55.8°(0.3°) | 55.4°(0.6°) | 55.8°(1.2°) | 55.0°(0.02°) |
| DOA 2 | 57.0°(0.3°) | 57.8°(0.5°) | 58.2°(1.2°) | 60.0°(0.02°) |

TABLE VI

THIRTEEN-ELEMENT DUALBAND UCA: MEAN AND STANDARD DEVIATION FOR DOA ESTIMATION AT 1800 MHz FOR INCOMING SIGNALS AT 55° AND 55° + $\delta$, WITH SNR=10dB.



## 2-D DOA estimation with UCAs

- **UCA-RARE DOA estimation in azimuth angle**
  - **Beamspace data correlation matrix**

$$\mathbf{R} = E\{\mathbf{x}_{beam}(t)\,\mathbf{x}_{beam}(t)^H\} = \mathbf{E}_S\,\mathbf{\Lambda}_S\,\mathbf{E}_S^H + \mathbf{E}_N\,\mathbf{\Lambda}_N\,\mathbf{E}_N^H$$

  - **Beamspace MUSIC function**

$$f_{MUSIC}(\theta,\varphi) = \mathbf{a}_{beam}^H(\theta,\varphi)\,\mathbf{E}_N\,\mathbf{E}_N^H\,\mathbf{a}_{beam}(\theta,\varphi)$$

  - **Factorization of array manifold**

$$\mathbf{a}_{beam}(\theta,\varphi) = \mathbf{T}(e^{j\varphi})\,\mathbf{g}(\theta)$$

$$z = e^{j\varphi}$$
$$[\mathbf{g}(\theta)]_k = \sin\theta\, V_{M-k+1}^l(\theta) \quad k = 1\ldots M+1, \quad \mathbf{T}(z) = \begin{bmatrix} \mathbf{Q}(z) & 0 \\ 0 & 1 \\ \mathbf{\Pi Q}(1/z) & 0 \end{bmatrix}$$
$$\mathbf{Q}(z) = diag\{z^{-M}, z^{-M+1}, \ldots, z^{-2}, z^{-1}\}$$

## 2-D DOA estimation with UCAs

- **UCA-RARE DOA estimation in azimuth angle**
  - Factorized beamspace MUSIC function

$$f_{MUSIC}(\theta,\varphi) = \mathbf{g}^H(\theta)\,\mathbf{T}^H(z)\,\mathbf{E}_N\,\mathbf{E}_N^H\,\mathbf{T}(z)\,\mathbf{g}(\theta)$$

  - $f_{MUSIC}$ = 0 at the required DOAs ($\theta$, $\phi$)
  - As $\theta$ is unknown, we solve the extended MUSIC function

$$f_{MUSIC}(\theta,\varphi) = \mathbf{c}^H\,\mathbf{T}^H(z)\,\mathbf{E}_N\,\mathbf{E}_N^H\,\mathbf{T}(z)\,\mathbf{c} = 0$$

  - Roots of the 1-D polynomial

$$P_{RARE}(z)_{|z|=1} = \det\left\{\mathbf{T}(1/z)^T\,\mathbf{E}_N\,\mathbf{E}_N^H\,\mathbf{T}(z)\right\} = 0$$

    yield the estimates for $\phi$
  - Spurious solutions also satisfy ( $\boldsymbol{\Delta} = (\mathbf{T}(1/z)^T\,\mathbf{T}(z))^{-1}$ )

$$P_{SPUR}(z)_{|z|=1} = \det\left\{\mathbf{E}_S^H\,\mathbf{T}(z)\,\boldsymbol{\Delta}\,\mathbf{T}(1/z)^T\,\mathbf{E}_S\right\} = 0$$



## 2-D DOA estimation with UCAs

- **root-MUSIC DOA estimation in elevation**
  - Extended array manifold to θ in [0, 2π]

$$b_t(\theta,\varphi) = \begin{cases} a_t(\theta,\varphi) & \text{for} \quad \varphi=[0,2\pi]\,,\ \theta=[0,\pi] \\ -a_t(2\pi-\theta,\pi+\varphi) & \text{for} \quad \varphi=[0,2\pi]\,,\ \theta=[\pi,2\pi] \end{cases}$$

  - Expansion as a double Fourier series ( $z = e^{j\varphi}$, $e^{jn\theta} = w^n$ )

$$b_t(\theta,\varphi) = \sum_{m=-M}^{M}\sum_{n=-N}^{N} f_{mn} z^m w^n e^{-jm\varphi_t}$$

  - Beamspace transformation of the extended manifold

$$\mathbf{b}_{beam}(\theta,\varphi) = \mathbf{W}\,\mathbf{b}(\theta,\varphi) = \boldsymbol{\Gamma}(\varphi)\,\mathbf{F}\,\mathbf{w}$$

$$[\mathbf{F}]_{m+M+1,n+N+1} = f_{mn}, [\mathbf{w}]_{n+N+1} = e^{jn\theta} = w^n \quad \boldsymbol{\Gamma}(\varphi) = \begin{bmatrix} z^{-M} & & \\ & \ddots & \\ & & z^{M} \end{bmatrix}$$

## 2-D DOA estimation with UCAs

- **root-MUSIC DOA estimation in elevation**
  - **MUSIC function cast in a form suitable for root-MUSIC**

$$f_{MUSIC}(\theta,\varphi) = \mathbf{w}^H \mathbf{Q}\,\mathbf{Q}^H \mathbf{w}$$

with $\mathbf{Q} = \mathbf{F}^H \boldsymbol{\Gamma}^H(\widehat{\varphi}_i)\,\mathbf{E}_N$ to be evaluated for each pair of estimates $\{\widehat{\varphi}_i, \widehat{\varphi}_i + \pi\}$

  - **Determination of the roots closest to the unit circle yields**

$$\begin{cases} \widehat{\theta}_s^i \in [0,\pi] \Longrightarrow (\widehat{\theta}_s^i, \widehat{\varphi}_i) \\ \widehat{\theta}_s^i \in [\pi,2\pi] \Longrightarrow (2\pi - \widehat{\theta}_s^i, \widehat{\varphi}_i + \pi) \end{cases}$$



## 2-D DOA estimation with UCAs

- **UCA-RARE/root-MUSIC with 9-dipoles UCA**

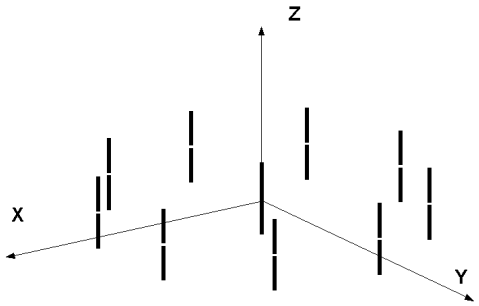


  - **frequency: 900 MHz**
  - **$Z_0$ =73Ω**
  - **10000-bit pseudo random bit sequences**
  - **Equal source power**

## 2-D DOA estimation with UCAs

### UCA-RARE/root-MUSIC with 9-dipoles UCA

- Three incoming signals with DOAs ($\theta$, $\phi$)
  signal 1: (120°, 0°), signal 2: (50°, 240°), signal 3: (70°, 115°)
- Mean and standard deviation of 500 implementations, for different SNR levels

| UCA-RARE + Root-MUSIC | | |
|---|---|---|
| 20dB | 10dB | 3dB |
| 120.01° (0.19°) | 120.09° (0.35°) | 120.08° (0.51°) |
| 0.01° (0.07°) | 0.02° (0.13°) | 0.05° (0.19°) |
| 49.95° (0.18°) | 49.94° (0.32°) | 49.95° (0.51°) |
| 240.00° (0.14°) | 240.01° (0.25°) | 240.03° (0.38°) |
| 69.95° (0.22°) | 69.94° (0.40°) | 69.89° (0.59°) |
| 115.00° (0.04°) | 115.00° (0.08°) | 115.00° (0.14°) |



## Performance of MIMO-systems

### Effect of antenna signal correlation in UCAs

- Spatial correlation between antenna signals at terminals $i$ and $j$
  - **Spatial variance between signals $V_i(\theta,\phi)$ and $V_j(\theta,\phi)$**

$$\sigma_s^2(i,j) = \int_{\phi=0}^{2\pi}\int_{\theta=0}^{\pi} V_i(\theta,\phi)V_j^*(\theta,\phi)f(\theta,\phi)\,d\phi\,\sin\theta\,d\theta$$

  - **Spatial correlation**

$$R_s(i,j) = \frac{\sigma_s^2(i,j)}{\sigma_s(i,i)\sigma_s(j,j)}$$

  - **Probability density function of angles of arrival $f(\theta,\phi)$**
    - uniform in azimuth plane
    - uniform over unit sphere
    - Laplacian

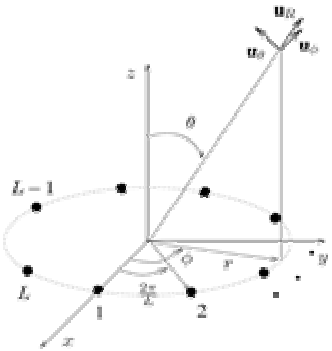

## Performance of MIMO-systems

- **Effect of antenna signal correlation in UCAs**
  - Laplacian probability density function of azimuth angle

$$f(\phi) = \frac{a}{2(1-e^{-a\pi})} e^{-a|\xi-\phi|},$$
$$-\pi + \xi < \phi < \pi + \xi,$$

$\xi$: main DOA

a: measure for angular spread

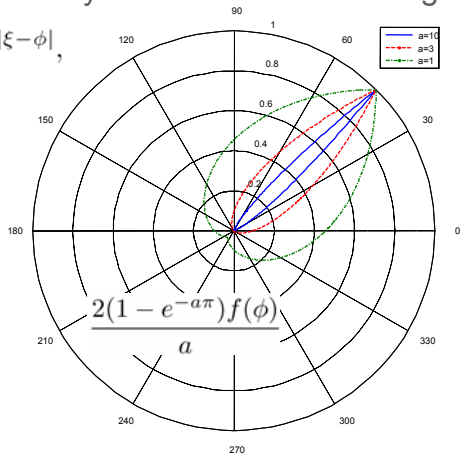




## Performance of MIMO-systems

- **Effect of antenna signal correlation in UCAs**
  - Spatial variance given a Laplacian distribution in azimuth plane
    - **Expressed as an expansion into phase modes**

$$\sigma_s^2(i,j) = \frac{a^2}{(1-e^{-a\pi})} \sum_{m=-M}^{+M} \sum_{n=-M}^{+M} \frac{Z_0}{Z_0 + Z_m^{\phi}} V_{0,m}^{\mathrm{V},\phi} e^{jm(\xi-\phi_i)}$$
$$\frac{Z_0^*}{Z_0^* + Z_n^{*\phi}} V_{0,n}^{*\mathrm{V},\phi} e^{-jn(\xi-\phi_j)} \frac{1-(-1)^{m-n}e^{-a\pi}}{a^2+(m-n)^2}$$

    - **Uniform DOA distribution in azimuth plane (a → 0)**

$$\sigma_s^2(i,j) = \sum_{m=-M}^{+M} \left| \frac{Z_0}{Z_0 + Z_m^{\phi}} \right|^2 \left| V_{0,m}^{\mathrm{V},\phi} \right|^2 e^{jm(\phi_j-\phi_i)}$$

    - **Correlation in absence of mutual coupling agrees with results in literature**

## Performance of MIMO-systems

- **Effect of antenna signal correlation in UCAs**
  - Spatial variance given a uniform distribution over the unit sphere
    - **Expressed as an expansion into spherical waves**
      - Vertically polarized incoming signals

$$\sigma^2_{s,H}(i,j) = \frac{\lambda^2}{\pi R_c^2} \sum_{m=-M}^{+M} \left| \frac{Z_0}{Z_0 + Z_m^\phi} \right|^2 \left\{ \sum_{n=1}^{+\infty} \frac{(n+|m|)!}{(n-|m|)!} \left[ |m| |A^{\phi,\theta}_{n,m}|^2 + \left( \frac{2n(n+1)}{(2n+1)} - |m| \right) |B^{\phi,\theta}_{n,m}|^2 \right.\right.$$
$$+ 2m \sum_{l=1}^{+\infty} \left( \Re(A^{\phi,\theta}_{n,m} A^{*\phi,\theta}_{n+2l,m}) + \Re(A^{\phi,\theta}_{n,m} B^{*\phi,\theta}_{n+2l-1,m}) \right.$$
$$\left.\left.\left. - \Re(A^{\phi,\theta}_{n+2l-1,m} B^{*\phi,\theta}_{n,m}) - \Re(B^{\phi,\theta}_{n+2l,m} B^{*\phi,\theta}_{n,m}) \right) \right] \right\} e^{jm(\phi_j - \phi_i)}$$

      – Horizontally polarized incoming signals

$$\sigma^2_{s,V}(i,j) = \frac{\lambda^2}{\pi R_c^2} \sum_{m=-M}^{+M} \left| \frac{Z_0}{Z_0 + Z_m^\phi} \right|^2 \left\{ \sum_{n=1}^{+\infty} \frac{(n+|m|)!}{(n-|m|)!} \left[ |m| |B^{\phi,\theta}_{n,m}|^2 + \left( \frac{2n(n+1)}{(2n+1)} - |m| \right) |A^{\phi,\theta}_{n,m}|^2 \right.\right.$$
$$+ 2m \sum_{l=1}^{+\infty} \left( \Re(B^{\phi,\theta}_{n,m} B^{*\phi,\theta}_{n+2l,m}) + \Re(B^{\phi,\theta}_{n,m} A^{*\phi,\theta}_{n+2l-1,m}) \right.$$
$$\left.\left.\left. - \Re(B^{\phi,\theta}_{n+2l-1,m} A^{*\phi,\theta}_{n,m}) - \Re(A^{\phi,\theta}_{n+2l,m} A^{*\phi,\theta}_{n,m}) \right) \right] \right\} e^{jm(\phi_j - \phi_i)}$$



## Performance of MIMO-systems

- **Effect of antenna signal correlation in UCAs**
  - Spatial variance given a uniform distribution in the azimuth plane

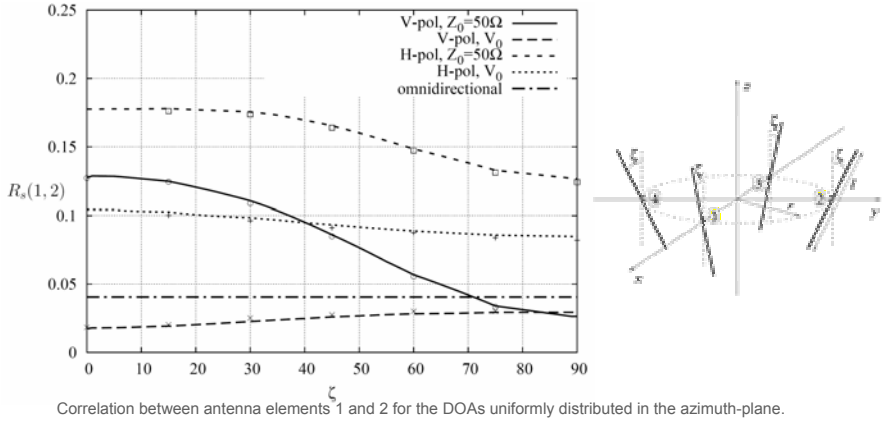


Correlation between antenna elements 1 and 2 for the DOAs uniformly distributed in the azimuth-plane.
Monte-Carlo simulation results: (◦): vertical polarization, $Z_0$ = 50Ω; (◇): vertical polarization, open-circuit voltages; (③): horizontal polarization, $Z_0$ = 50Ω; (+): horizontal polarization, open-circuit voltages.

## Performance of MIMO-systems

- **Effect of antenna signal correlation in UCAs**
  - Spatial variance given a Laplacian distribution in azimuth plane

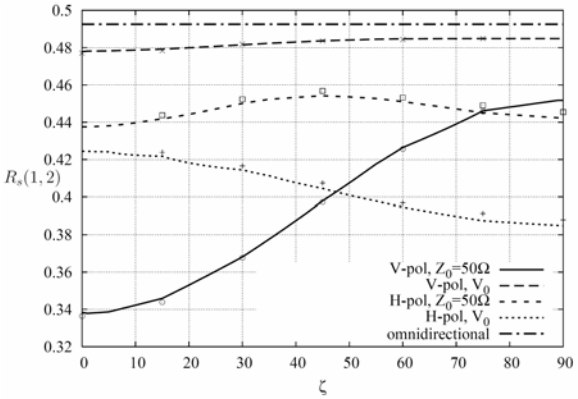


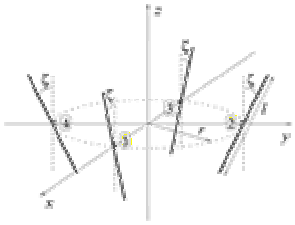

Correlation between antenna elements 1 and 2 for Laplacian distribution (a = 3, ξ= 0°) of DOAs in the azimuth-plane. Monte-Carlo simulation results: (◦): vertical polarization, $Z_0$ = 50Ω; (◈): vertical polarization, open-circuit voltages; (③): horizontal polarization, $Z_0$ = 50Ω; (+): horizontal polarization, open-circuit voltages.



## Performance of MIMO-systems

- **Effect of antenna signal correlation in UCAs**
  - Spatial variance given a uniform distribution over the unit sphere

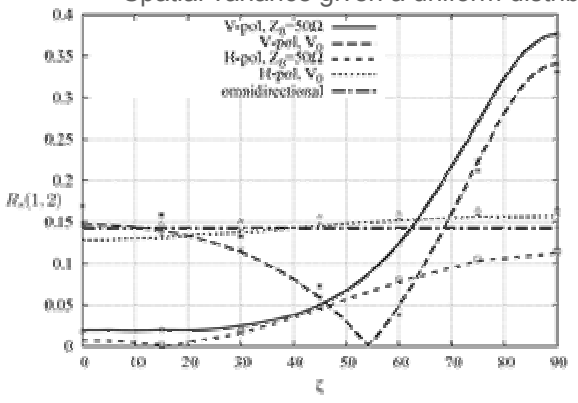


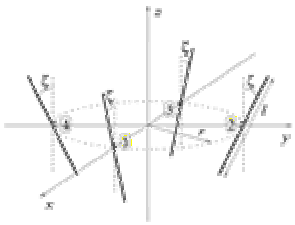

Monte-Carlo simulation results: (◦): vertical polarization, $Z_0$ = 50Ω; (◈): vertical polarization, open-circuit voltages; (∗): vertical polarization, open-circuit voltages of standalone antenna elements, no mutual coupling; (③): horizontal polarization, $Z_0$ = 50Ω; (+): horizontal polarization, open-circuit voltages; (⇔): horizontal polarization, open-circuit voltages of stand-alone antenna elements, no mutual coupling.

## Performance of MIMO-systems

- **Effect of correlation on channel capacity**
  - Antenna signal correlation affects mean (ergodic) channel capacity <C>, because of upper bound

$$\langle C \rangle \leq \overline{C} = \log_2 \det \left[ \overline{\overline{I}} + \frac{\rho}{L} \overline{\overline{R}} \right]$$

with $\overline{\overline{R}} = [R_s(i,j)]$ correlation matrix,
$\rho$ / L: average signal-to-noise ratio in each of the L antennas.

  - $\overline{C}$ = capacity of the mean channel
  - Maximum capacity corresponds to uncorrelated antenna elements $\overline{\overline{R}} = \overline{\overline{I}}$

$$C_{\max} = L \log_2 \left(1 + \frac{\rho}{L}\right)$$



## Performance of MIMO-systems

- **Effect of correlation on channel capacity**

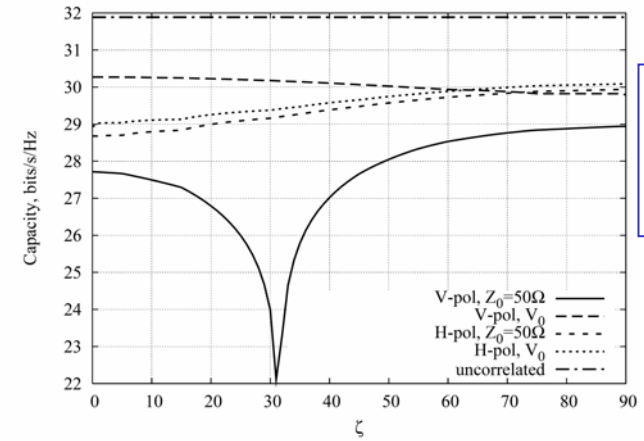


*Reduced channel capacity due to antenna coupling (spatial correlation)*

Capacity of the mean channel, for a Laplacian distribution (a = 3, ξ= 0°) of DOAs in the azimuth-plane, and for ρ = 30dB, L = 4

## Design of wearable antennas

- ***Personal Health* and *Ambient Assisted Living* applications require wireless communication link**
  - Wireless body area networks (WBANs)
  - Wireless personal area networks (WPANs): Bluetooth [1] (IEEE 802.15), WiFi (IEEE 802.11b/g), Wireless USB, and WiMAX (IEEE 802.16a)
  - Wireless sensor networks: Zigbee
- ***Wearable computing* systems provide high functionality, without disturbing comfort and mobility of the person wearing it**
- **Textile antennas are flexible, compact and easily integratable into clothing**
- **Use of novel electrotextiles together with careful antenna design provide textile antenna efficiency required for robust low-power communications**



## Design of wearable antennas

- **Planar antennas most suited**
- **Presence of ground plane shields antenna radiation from body**
- **Suitable choice of textile materials**
  - Electrotextiles acting as antenna plane and ground plane
    - **High conductivity required**
      **→ Skin-effect at microwave frequencies!**
  - Non-conducting textiles acting as substrate
    - **Sufficiently thick to provide sufficient bandwidth and antenna efficiency (few mm)**
    - **Permittivity close to one (garment should mainly consist of air)**
    - **Low water content to keep losses low**
- **Accurate characterization of EM properties of textiles is an issue!**

## Design of wearable antennas

- **Rectangular-ring textile antenna**
  - Covering [2.4-2.485 GHz] ISM band
  - Robust to bending
  - (nearly) circular polarization

| *patch (Flectron®)* | | *substrate (Fleece)* | |
|---|---|---|---|
| $L$ [mm] | 49 | $h$ [mm] | 2.56 |
| $W$ [mm] | 52 | $\varepsilon_r$ | 1.25 |
| Feed point [mm] | (7;9) | tan $\delta$ | 0 |
| *Slot* | | | |
| $l$ [mm] | 8 | | |
| $w$ [mm] | 7 | | |

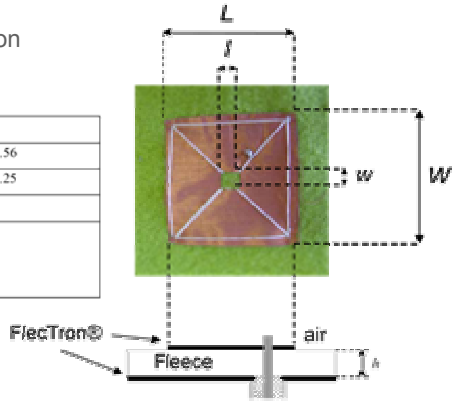




## Design of wearable antennas

- **Measured and simulated return loss**
  - Design bandwidth large enough to provide robust antenna characteristics in presence of bending

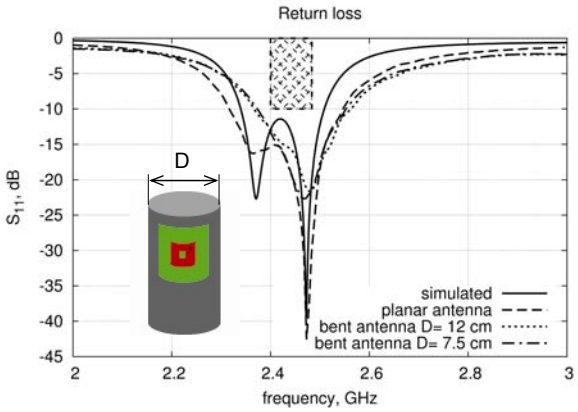


- bandwidth without bending: [2.34 – 2.51 GHz]
- in-band return loss < -11.2 dB
- excitation of two orthogonal modes provides extra robustness

## Design of wearable antennas

- **Simulated antenna gain at 2.45 GHz**
  - Design bandwidth large enough to provide robust antenna characteristics in presence of bending

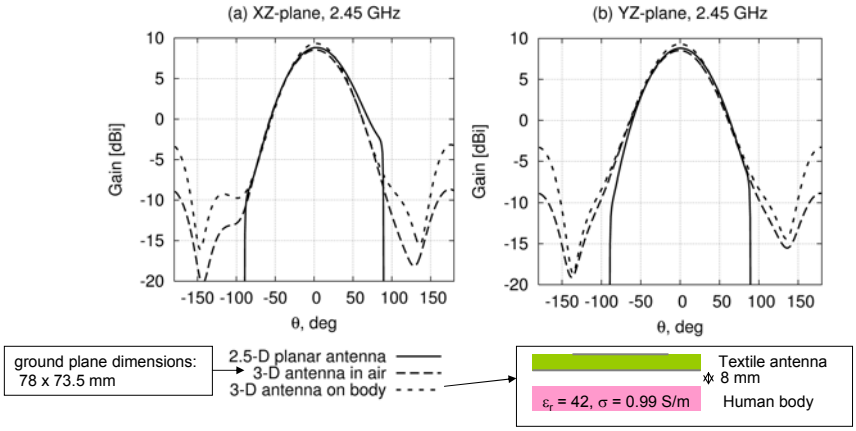




## Design of wearable antennas

- **Measured antenna gain along broadside direction**
  - Measured antenna efficiency at least 70%
  - No significant decrease in gain when receive antenna is rotated with respect to transmit antenna

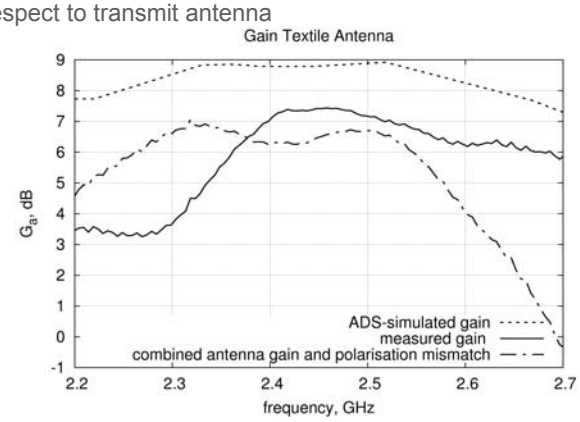

## Selected list of publications


- H. Rogier and D. De Zutter, “Beamforming Strategies for Compact Arrays Using the Exact Active Element Pattern Method,” Microwave and Optical Technology Letters, vol. 35, no. 3, pp. 202–203, Nov. 2002.
- H. Rogier and D. De Zutter, “Prediction of noise and interference cancellation with a moving compact receiver array in an indoor environment,” IEEE Trans. Vehicular Technology vol. 54, no. 1, pp. 191–197, Jan. 2005.
- H. Rogier, “Phase-mode Based Construction of a Coupling Matrix for Uniform Circular Arrays with a Center Element," Microwave Opt. Technol. Lett., vol. 48, no. 2 pp. 291-298, Feb. 2006.
- A. Tronquo, H. Rogier, C. Hertleer and L. Van Langenhove, “A Robust Planar Textile Antenna for Wireless Body LANs Operating in the 2.45-GHz ISM band,” IEE Electronics Letters, vol. 42, no. 3, pp. 142–143, Feb. 2006.
- H. Rogier and E. Bonek, “Analytical Spherical-Mode Based Compensation of Mutual Coupling in Uniform Circular Arrays for Direction-of-Arrival Estimation,” International Journal of Electronics and Communications, vol. 60, pp. 179–189, Mar. 2006.
- H. Rogier, “Spatial Correlation in Uniform Circular Arrays based on a Spherical-Waves Model for Mutual Coupling," International Journal of Electronics and Communications, in press, 2006.
- R. Goossens and H. Rogier, “2-D Direction of Arrival Estimation Combining UCA-RARE and MUSIC for Uniform Circular Arrays Subject to Mutual Coupling,” Proc. Int. Conf. on Electromagnetics in Advanced Applications, pp. 791–794, Sept. 2005.

# Second Workshop on Advanced Computational Electromagnetics

## Ghent – May 3-4, 2006

***- Program -***

### Wednesday, May 3, 2006

8h30 Welcome

9h00 Andreas Cangellaris, University of Illinois at Urbana-Champaign, USA
*Model Order Reduction of Finite Element Models of Electromagnetic Systems Using Krylov Subspace Methods*

10h30 Coffee Break

10h45 Dominique Lesselier, Supélec, France
*3-D Electromagnetic Inverse Scattering Methodologies with Emphasis on the Retrieval of Small Objects*

12h15 Lunch

14h00 Rob Remis, Delft University of Technology, The Netherlands
*Low- and High-Frequency Model-Order Reduction of Electromagnetic Fields*

15h30 Coffee Break

15h45 Hendrik Rogier, Ghent University, Belgium
*State-of-the-art Antenna Systems in Mobile Communications*

### Thursday, May 4, 2006

8h30 Welcome

9h00 Andreas Cangellaris, University of Illinois at Urbana-Champaign, USA
*Comprehensive Electromagnetic Modeling of On-Chip Noise Generation and Coupling During High Speed Switching*

10h30 Coffee Break

10h45 Davy Pissoort, Ghent University, Belgium
*Fast and Accurate Modeling of Photonic Crystal Devices*

12h15 Lunch

14h00 Tom Dhaene, University of Antwerp, Belgium
*Electromagnetic-Based Scalable Metamodeling*

15h30 Coffee Break

15h45 Luc Knockaert, Gunther Lippens, and Daniël De Zutter, Ghent University, Belgium
*Towards a Classification of Projection-Based Model Order Reduction*

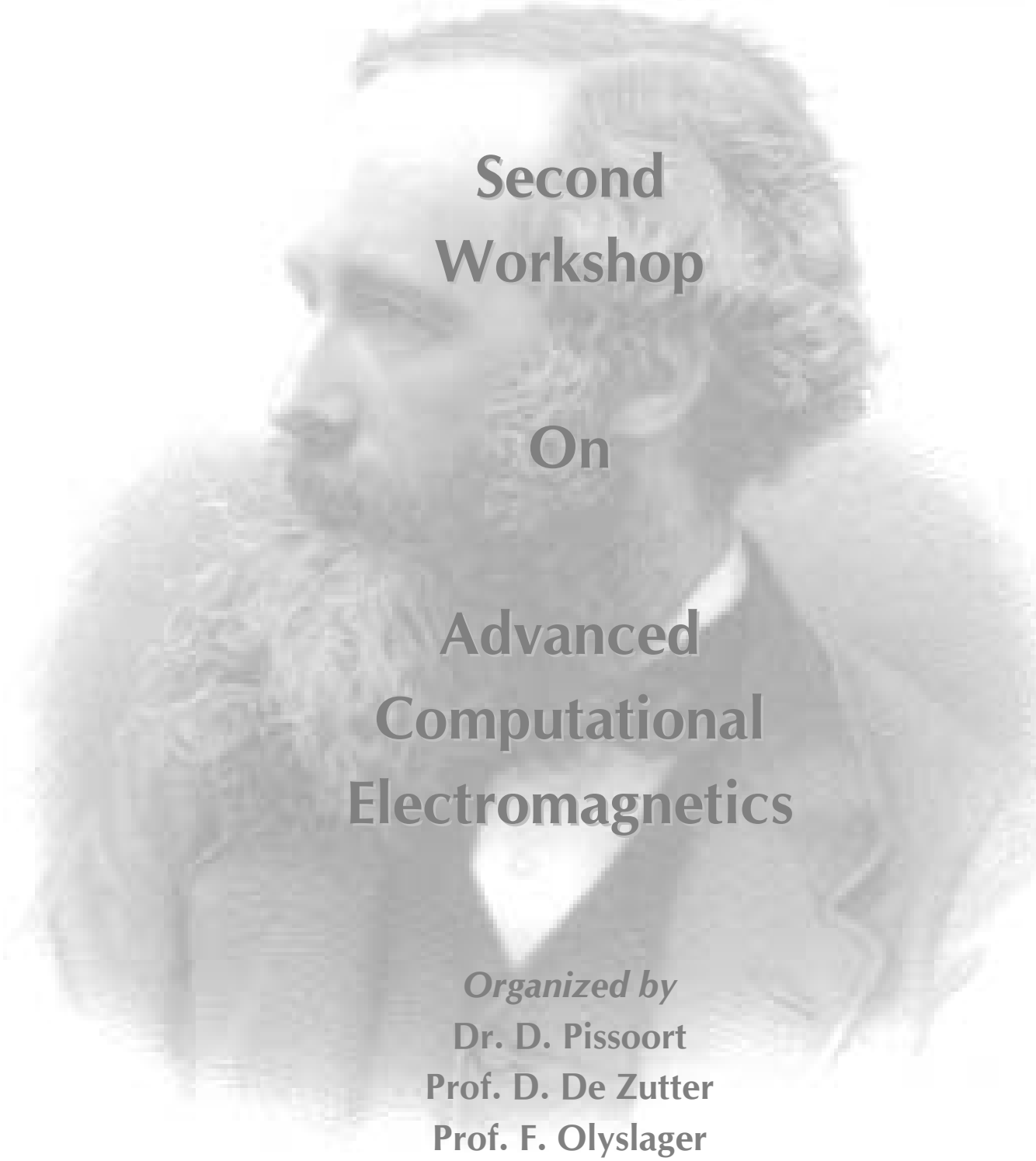

# Second Workshop

# On

# Advanced Computational Electromagnetics

*Organized by*

Dr. D. Pissoort
Prof. D. De Zutter
Prof. F. Olyslager
Prof. A. Franchois